

## Structural changes induced by Ce filling in partially filled skutterudites

This article has been downloaded from IOPscience. Please scroll down to see the full text article.

2005 J. Phys.: Condens. Matter 17 3525

(<http://iopscience.iop.org/0953-8984/17/23/005>)

View [the table of contents for this issue](#), or go to the [journal homepage](#) for more

Download details:

IP Address: 129.252.86.83

The article was downloaded on 28/05/2010 at 04:58

Please note that [terms and conditions apply](#).

# Structural changes induced by Ce filling in partially filled skutterudites

L C Chapon<sup>1</sup>, L Girard<sup>2</sup>, A Haidoux<sup>2</sup>, R I Smith<sup>1</sup> and D Ravot<sup>2</sup>

<sup>1</sup> ISIS facility, Rutherford Appleton Laboratory-CCLRC, Chilton, Didcot, Oxfordshire OX11 0QX, UK

<sup>2</sup> LPMC, UMR 5617 CNRS, CC03, Université Montpellier II, 5 place E. Bataillon, 34095 Montpellier Cedex 05, France

Received 7 February 2005, in final form 9 May 2005

Published 27 May 2005

Online at [stacks.iop.org/JPhysCM/17/3525](http://stacks.iop.org/JPhysCM/17/3525)

## Abstract

The structural properties of the  $\text{Ce}_\delta\text{Fe}_{4-x}\text{Ni}_x\text{Sb}_{12}$  series with  $0.06 \leq \delta \leq 0.72$  have been determined by neutron powder diffraction in the temperature range 10–300 K. Large isotropic atomic displacement parameters are observed for the cerium atom throughout the series, however with two distinct origins. The first term, purely dynamic, is well described as an Einstein oscillator and has essentially no dependence with the filling fraction  $\delta$  and the lattice parameter. A vibrational frequency of  $55(2) \text{ cm}^{-1}$  fitted the experimental data in the entire phase diagram. The second contribution is essentially static and well evidenced by a large residual displacement parameter extrapolated to 0 K. This latter term does depend strongly on  $\delta$  and is maximum at around  $\delta = 0.5$ , representing almost 50% of the room temperature value. A number of structural changes of the Sb sublattice are correlated with the disorder of Ce as well as disorder on the Fe/Ni sublattice.

## 1. Introduction

Rare-earth filled skutterudites (of formula  $\text{RM}_4\text{X}_{12}$  where R is a rare-earth atom, M a transition element and X a pnictogen) have attracted a lot of interest because of their rich physical properties inherent to the presence of f electrons. Moreover, filled skutterudites have been extensively studied in view of their high thermoelectric efficiency since it was shown that the electronic and thermal properties of these materials can be somehow decoupled [1]. Originally, Slack [2] proposed that semiconductors whose crystal structures offer large open spaces should be ideal candidates for the realization of high thermoelectric figures of merit. When heavy atoms fill the voids of such structures, they undergo large vibrations (usually referred to as ‘rattling’) due to a weak bonding with the ‘host’ network. These low energy localized vibrational modes interact with the acoustic phonons primarily responsible for the heat conduction. Consequently, the lattice thermal conductivity ( $\kappa_l$ ) is greatly reduced with respect to those of unfilled analogues whereas the electronic properties are substantially less affected

by the presence of the *rattlers*. Even though the picture of the rattler seems oversimplified [3] and the exact mechanisms are still unclear, the thermal conductivities measured for a variety of filled skutterudites [4–7] are as low as  $10 \text{ mW cm}^{-1} \text{ K}^{-1}$  at room temperature, i.e. an order of magnitude lower than for unfilled compounds.

Among all the techniques, diffraction study has probably given the clearest evidence that heavy ions filling the voids of the so-called open cage structures undergo large vibrations, through the systematic observation of large atomic displacement parameters (ADP) [8, 9]. Also, vibrational frequencies extracted from the temperature dependence of the ADP are in excellent agreement with the results obtained with Raman, inelastic neutron scattering [10] or x-ray absorption fine structure (EXAFS) measurements [11].

For filled and partially filled skutterudites, where  $\kappa_1$  shows a peak at low temperature [12], the thermal properties are reminiscent of crystals and therefore the possibility of tunnelling as proposed for the clathrates [8] is excluded. Nonetheless, it is still unclear what role is played by disorder in these systems. In particular the lattice thermal conductivities of partially filled skutterudites are systematically lower than those of totally filled ones [4–7]. Mass fluctuation scattering has been considered as the main reason for the drop observed but leads to conflicting results in the calculation of  $\kappa_1$  [6, 7]. Meanwhile, several structural studies have shown that the static disorder of the rare-earth ions in partially filled skutterudites is significant [5, 9, 13]. Of note is a recent work by Feldmann *et al* [14] that revealed a large broadening of Raman peaks for a La partially filled sample and led these authors to conclude that these features are probably due to disorder. Although positional disorder of the R ions and potential relaxation of the M–X covalent network around empty R sites is believed to play a role in the thermal properties of partially filled skutterudites, the lack of structural information on a broad range of compositions has meant that a comprehensive investigation into these effects has not been possible. In this paper, we report on a detailed neutron powder diffraction study of the  $\text{Ce}_\delta\text{Fe}_{4-x}\text{Ni}_x\text{Sb}_{12}$  series where the structural parameters have been mapped out for nine samples in the range  $0.06 \leq \delta \leq 0.72$  between 10 and 280 K. In addition to the large Ce ADP found near  $\delta = 0.5$  as a consequence of static disorder, it is found that the Sb sublattice is substantially affected by the presence of Ce and by positional disorder effects. The variation of the anisotropic Sb ADP tensor with  $\delta$  gives precious insight into the nature of the Ce–Sb interaction.

## 2. Experiment

Polycrystalline samples of  $\text{Ce}_\delta\text{Fe}_{4-x}\text{Ni}_x\text{Sb}_{12}$  with  $0.06 \leq \delta = (4 - 2x)/3 \leq 0.72$  were synthesized directly from the elements at high temperature. Granules of Ce (99.9% Aldrich), Fe (99.9999% Alfa), Ni (99.9999% Aldrich) and Sb (99.9999% Alfa) were mixed in the appropriate stoichiometry and sealed under a pressure of less than  $10^{-5}$  mbar in quartz ampoules. The ampoules were heated at 1273 K for 48 h in a vertical furnace, water quenched and then annealed at 973 K for five days. Small portions of the ingots were cut for preliminary analysis by x-ray powder diffractometry and scanning electron microscopy. All the samples were found to be very pure with the exception of the ones corresponding to  $\delta = 0.06$  and 0.16 for which small amounts of  $(\text{Fe, Ni})\text{Sb}_2$  were detected ( $\leq 5\%$ ). Time-of-flight neutron powder diffraction data were collected on the POLARIS diffractometer at the ISIS facility, Rutherford Appleton Laboratory (UK). The samples ( $\sim 5$  g per composition) were finely ground and sieved to  $10 \mu\text{m}$  to minimize extinction issues during the Rietveld refinements and were loaded into vanadium cans sealed under helium atmosphere. All measurements were performed on warming from 10 to 280 K using a closed-cycle refrigerator. Temperature steps of 10, 20 and 40 K were chosen in the temperature ranges 10–110, 110–200 and 200–280 K, respectively.

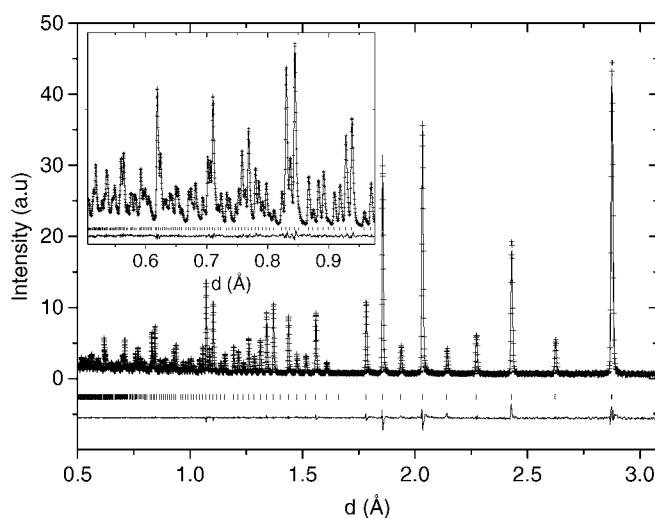


**Figure 1.** Observed (cross symbol) and calculated (continuous line) diffraction patterns for  $\text{Ce}_{0.5}\text{Fe}_{2.75}\text{Ni}_{1.25}\text{Sb}_{12}$  at room temperature (backscattering bank of detectors,  $2\theta = 145^\circ$ ). The solid line at the bottom represents the difference between observed and calculated patterns. The row of markers indicates the positions of Bragg reflections.

The collection time was 20 min at each temperature, ensuring high quality diffraction patterns (see figure 1 and table 1 for agreement factors). For each data set, the patterns collected in two detector banks situated at  $2\theta = 145^\circ$  and  $90^\circ$  were used simultaneously to refine the crystal structures with the Rietveld package GSAS [15]. Because it was essential that refined unit cell parameters be both accurate and self-consistent, corrections for sample displacement were made by carrying out a constrained refinement of the diffractometer constant (DIFC)<sup>3</sup> values calculated from geometrical considerations [16]. Sample absorption was refined using a Debye–Scherrer correction model. For compositions  $\delta = 0.06$  and  $0.16$ , extra reflections characteristic of the phase  $(\text{Fe}, \text{Ni})\text{Sb}_2$  were observed. Though this phase was added to the refinements, the fractional occupancies of Fe and Ni were not refined due to the similar nuclear scattering lengths of these elements ( $b(\text{Fe}) = 0.95$  fm,  $b(\text{Ni}) = 1.03$  fm) and were fixed at 0.5.

### 3. Results and discussion

It was shown [17] that partially filled skutterudites of the type  $\text{Ce}_\delta\text{Fe}_{4-x}\text{Ni}_x\text{Sb}_{12}$  can be synthesized in a large composition range ( $0 \leq \delta \leq 0.9$ ), providing a unique opportunity to study the effect of rare-earth filling on the structure of skutterudites (similarly Co can be substituted for Fe; see for example [4]). Interestingly these quaternary skutterudites can be isoelectronic to the semiconductor binary skutterudite  $\text{CoSb}_3$  when  $x$  and  $\delta$  are related by  $\delta = (4 - 2x)/3$  ( $\delta = (4 - x)/3$  in the case of Co substitution [4]). However, it was established that the Ce concentration is intimately connected to the Fe–Ni ratio [17] (Fe–Co ratio [4]) and that for high Fe content,  $\delta$  is significantly lower than calculated from the previous equation. Here, measurements have been made on nine compositions equally spaced between  $x = 0.65$  and 1.85. The Ce site occupancies have been refined from the room temperature diffraction

<sup>3</sup> The parameter DIFC (labelled as such in GSAS) is defined by  $\text{DIFC} = \frac{2mL \sin(\theta)}{h}$  where  $m$  is the neutron mass,  $L$  the total flight path,  $\theta$  the average angle of the detectors bank and  $h$  Planck's constant.

**Table 1.** Selected structural parameters for  $\text{Ce}_{0.5}\text{Fe}_{2.75}\text{Ni}_{1.25}\text{Sb}_{12}$  extracted from the Rietveld refinement at 10 K. Agreement factors are given.

Atoms	<i>x</i>	<i>y</i>	<i>z</i>
Ce	0	0	0
Fe/Ni	0.25	0.25	0.25
Sb	0	0.335 90(4)	0.158 83(4)
Thermal parameters × 100 (Å <sup>2</sup> )			
Ce	<i>U</i> <sub>iso</sub> : 1.25(6)		
Fe/Ni	<i>U</i> <sub>iso</sub> : 0.225(4)		
Sb	<i>U</i> <sub>11</sub> : 0.201(9)	<i>U</i> <sub>22</sub> : 0.545(16)	<i>U</i> <sub>33</sub> : 0.145(15)
	<i>U</i> <sub>12</sub> : 0	<i>U</i> <sub>13</sub> : 0	<i>U</i> <sub>23</sub> : 0.055(8)
Lattice parameter (Å)	9.085 97(2)		
Agreement factors:			
<i>R</i> <sub>F<sup>2</sup></sub> (%)	1.3 (145° bank)	2.2 (90° bank)	
<i>R</i> <sub>wp</sub> (%)	2.4 (145° bank)	3.6 (90° bank)	
Reduced $\chi^2$	1.16		

patterns to avoid systematic errors when refining the ADP and fixed to these values for Rietveld refinements at lower temperatures. It was found that  $\delta$  varies between 0.06 and 0.72 as indicated in figure 3(d). For high Fe content,  $\delta$  deviates substantially from  $\delta = (4 - 2x)/3$  (figure 3(d)) in agreement with measurements of the electrical resistivity showing a metallic behaviour for these samples [17]. Note that because quaternary compositions are needed to study the effect of void filling over a large range of  $\delta$ , one needs to take the Fe/Ni substitution into account when discussing the structural properties of the series.

Before going any further, the structure of the filled skutterudites (space group  $Im\bar{3}$ , No 204) as represented in figure 2 is described briefly. It consists of a three-dimensional network of corner-sharing distorted  $\text{MSb}_6$  octahedra ( $M = \text{Fe}, \text{Ni}$ ). The  $\overline{\text{MSbM}}$  interoctahedral bridging angle of  $\sim 127^\circ$  is much smaller than that found for example in the perovskite structure ( $\overline{\text{MOM}}$  close to  $180^\circ$ ). As a consequence of this strongly tilted arrangement two large voids per unit cell located at the  $(0, 0, 0)$ ,  $(\frac{1}{2}, \frac{1}{2}, \frac{1}{2})$  position (site 2(a)) can be filled by the Ce atom. The Ce atom is 12-coordinated to the Sb atoms with a distorted icosahedral geometry ( $T_h$  point symmetry). Another unique feature of the skutterudite structure, resulting from the tilted arrangement of corner-linked octahedra, is the presence of rectangular  $\text{Sb}_4$  rings (figure 2). Within the rings, the shorter bond distance labelled Sb–Sb(1) in figure 2 connects atoms of the same Ce– $\text{Sb}_{12}$  polyhedron whereas the longer one, Sb–Sb(2), connects atoms belonging to adjacent polyhedra.

All compounds investigated were found to crystallize with the structure explained previously over the entire temperature range 10–300 K (see figure 1 for the agreement between experimental data and Rietveld refinement). The absence of superlattice reflections indicated that the Ce/vacancy and Fe/Ni sublattices remain disordered at all temperatures and for all compositions. Also no magnetic Bragg peaks were observed at low temperature, in agreement with the magnetic susceptibility measurements showing a paramagnetic behaviour down to 1.8 K [18]. Selected structural parameters extracted from the Rietveld refinements at 280 K are displayed in figure 3. The lattice parameter (figure 3(a)) expands by 0.03 Å as a function of composition ( $\Delta a/a = 0.32\%$  between end members of the series), a weak variation accounted for by several structural changes. As the Fe concentration increases, the M–Sb ( $M = \text{Fe}, \text{Ni}$ )

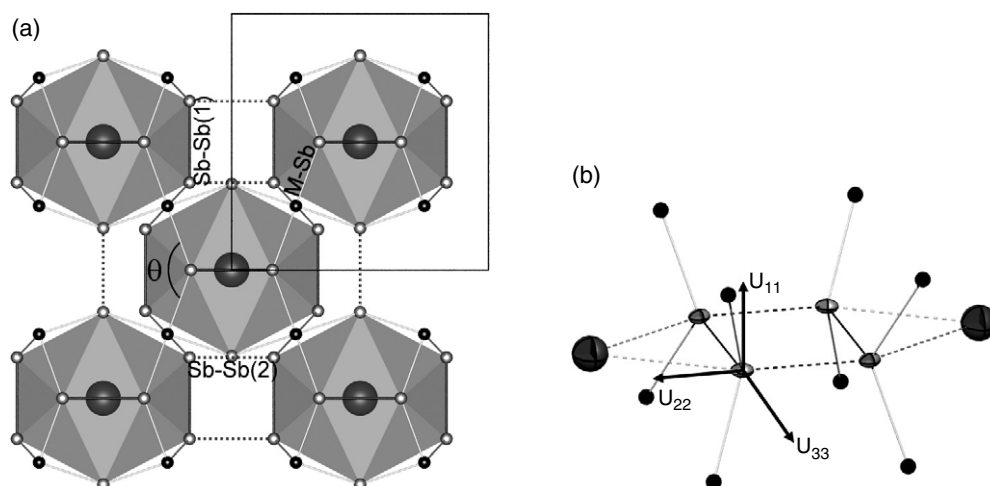


**Figure 2.** (a) Structure of a totally filled skutterudite (Ce: large grey sphere, (Fe, Ni): dark sphere and Sb: light grey sphere). CeSb<sub>12</sub> polyhedra are shown as transparent grey solids. The solid line marks the Bravais unit cell. (b) ORTEP representation of the ADPs for a filled skutterudite showing the three main components of the Sb thermal ellipsoid.  $U_{22}$  and  $U_{33}$  are the in-plane components within the Sb<sub>4</sub> rings.  $U_{11}$  is perpendicular to the Sb<sub>4</sub> plane.

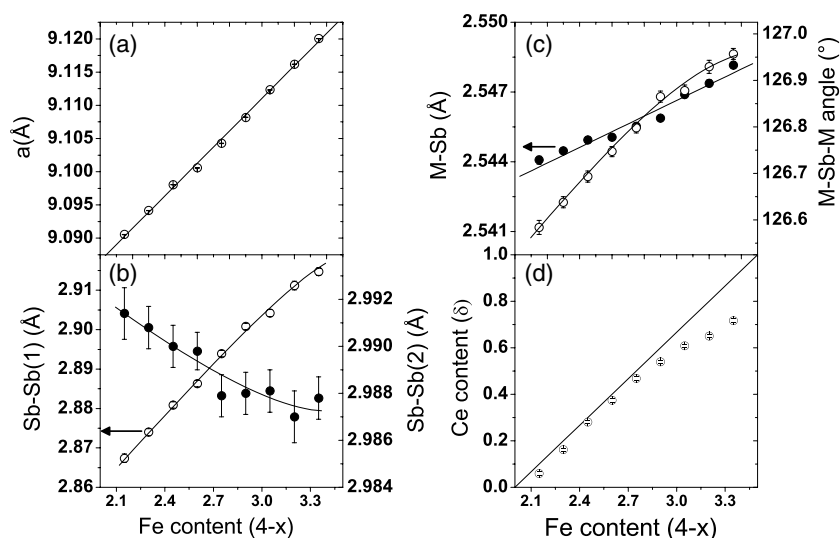


**Figure 3.** Selected structural parameters versus Fe content ( $4 - x$ ) for  $\text{Ce}_\delta\text{Fe}_{4-x}\text{Ni}_\delta\text{Sb}_{12}$  (see figure 2 for labels). (a) Lattice parameter. (b) Sb-Sb interatomic distances. (c) M-Sb interatomic distance (M = Fe, Ni) and M-Sb-M angle. (d) Refined Ce concentration. Solid lines are guides to the eyes except for part (d) for which the  $y = (4 - 2x)/3$  curve is displayed.

bond distance increases (figure 3(c)) while the interatomic distances within the Sb<sub>4</sub> rings show contrasting behaviours. Sb-Sb(1) increases with increasing Fe concentration while the Sb-Sb(2) distance decreases slightly, as indicated in figure 3(b). Finally, the M-Sb-M angle increases with increasing Fe concentration. Because  $\delta$  does not vary linearly with  $x$ , it is obvious from the shape of the curves in figure 3 that we could ascribe the observed variations

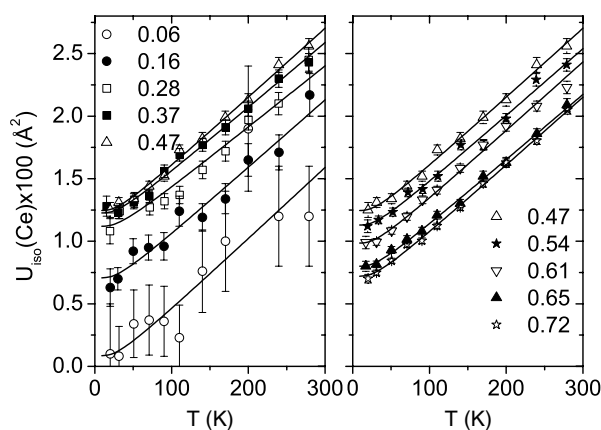


**Figure 4.** Temperature dependence of the Ce isotropic atomic displacement parameter for  $\text{Ce}_x\text{Fe}_{4-x}\text{Ni}_x\text{Sb}_{12}$ . The lines are fits of the data with equation (1) (see the text for details). The measured Ce filling fractions are displayed with corresponding symbols.

either to the effect of Fe/Ni substitution or to cerium filling. The linear dependence of the M–Sb distance with  $x$  shows that it is correlated with the Fe/Ni substitution and is consistent with larger ionic radii for Fe than for Ni. On the other hand the variations of all other parameters show a pronounced curvature at large Fe content that mimics the variation of  $\delta$  and therefore are correlated with the cerium concentration. The filling of the voids with cerium tends to enlarge the Sb–Sb(1) distance, but have only a minor effect on the Sb–Sb(2) distance. As a result the M–Sb–M angle increases, i.e. the interoctahedra tilting angle is reduced as a consequence of filling. The lattice parameter increases monotonically with  $x$  as a result of the combined effects described above.

Atomic displacement parameters of Ce, (Fe, Ni) and Sb have been extracted from the Rietveld refinements of data in the temperature range 10–280 K and are displayed in figures 4, 6 and 8. The Ce ADP tensor<sup>4</sup> ( $U_{ij}$ ,  $j = 1, 3$ ) is isotropic due to the cubic symmetry of the site. For the (Fe, Ni) site,  $U_{11} = U_{22} = U_{33}$  and the off-diagonal term ( $U_{12} = U_{13} = U_{23}$ ) was found to be essentially 0 within the error bar in the entire temperature range so that an isotropic treatment remains an excellent approximation. For the Sb ADP tensor, the four non-zero terms have been refined ( $U_{11}$ ,  $U_{22}$ ,  $U_{33}$  and  $U_{23}$ ). The results obtained at 280 K are in excellent agreement with data obtained previously for various filled skutterudites on single-crystal [9] and polycrystalline materials [5, 13]. Qualitatively, the main characteristic of these systems is the anomalously high ADP for the Ce atom, clear evidence of the large dynamical motion which was first discussed by Chakoumakos *et al* [9]. This is in contrast with lower ADP values observed for the other atoms of the structure due to a strong bonding occurring in the ‘host’ network. Quantitatively however, it is not straightforward to relate the Ce ADPs observed at room temperature to meaningful physical parameters. Only the temperature dependence reported in figure 4 allows a proper deconvolution of different contributions: when the temperature is lowered, the Ce ADP decreases as expected, at least in the harmonic approximation, and saturates for most samples to a value much larger than expected from zero-point motion alone. This behaviour shows the existence of static disorder, a term due to positional disorder as well as relaxation effects in disordered alloys. That contribution is

<sup>4</sup> The Debye–Waller factor  $T$  for an  $(hkl)$  reflection is related to the anisotropic displacement parameters by  $T(h, k, l) = \exp(h^2 a^{*2} U_{11} + k^2 b^{*2} U_{22} + l^2 c^{*2} U_{33} + 2hka^* b^* U_{12} + 2hla^* c^* U_{13} + 2klb^* c^* U_{23})$  where  $a^*$ ,  $b^*$ ,  $c^*$  are the reciprocal lattice parameters.

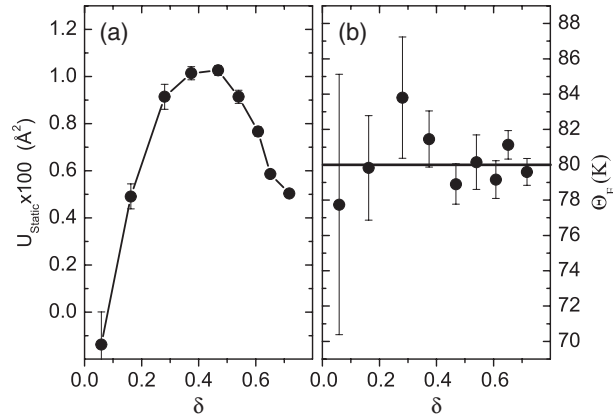


**Figure 5.** (a) Static disorder of Ce for  $\text{Ce}_\delta\text{Fe}_{4-x}\text{Ni}_x\text{Sb}_{12}$ . (b) Einstein temperature versus measured Ce filling fractions. The lines are guides to the eyes.

essentially temperature independent and therefore can be easily separated from the dynamic part of the displacement parameter. The temperature dependence of the Ce ADP has been approximated as the sum of a static term and an Einstein oscillator function [11, 13]:

$$U(T) = U_{\text{Static}} + \frac{h}{8\pi^2 m \nu} \coth\left(\frac{h\nu}{2k_{\text{B}}T}\right) \quad (1)$$

where  $U_{\text{Static}}$  is the static root mean square (rms) displacement parameter,  $h$  and  $k_{\text{B}}$  are respectively the Planck and Boltzmann constants,  $\nu$  the Einstein oscillator frequency and  $m$  the atomic mass of Ce. The Einstein model is an excellent approximation in this case because the rare-earth vibrations have very flat dispersion in skutterudites [3]. Also it was established that the harmonic approximation remains valid up to large Ce displacement [3]. A least-squares fit to the data with this function reveals that within the error bars, the Einstein frequency does not depend on the Ce filling fraction (figure 5) or the lattice parameter. An Einstein temperature ( $\Theta_{\text{E}}$ ) of 80(3) K is found over the entire temperature range as displayed in figure 5. This energy agrees extremely well with values extracted from inelastic neutron scattering [10] and recent EXAFS experiments [11] and values calculated from lattice dynamics for totally filled samples [3] (both found 80 K). In particular, this is slightly smaller (about 15%) than the ‘bare’ vibrational frequency calculated and supports the idea that the rare-earth modes are hybridized to the Sb modes. The dependence on the filling fraction is also consistent with the recent work on thallium filled skutterudites showing that the energy of the Tl localized modes determined by inelastic neutron scattering does not shift as the Tl concentration varies [19] (or within the error bar).

As expected, the static disorder depends strongly on the Ce filling fraction (figure 5) with maxima at around  $\delta = 0.5$  (for an ideal system, the static disorder will follow a curve  $U_{\text{static}} = \delta(1 - \delta)$ : solid line, inset to figure 6). At  $\delta = 0.5$ , the static disorder exceeds  $0.01 \text{ \AA}^2$  and represents almost 50% of the room temperature ADP. Assuming that relaxation effects are weak enough that we can relate the static disorder entirely to positional disorder, this value represents an average displacement of about  $0.1 \text{ \AA}$  from the Ce special position. This displacement is substantial for such a heavy element. We will note that the nuclear density found in difference Fourier maps where the Ce atom has been excluded from the calculation remains spherical even for  $\delta = 0.5$ . This result indicates that the possibility of a multi-well potential as observed for some thermoelectric clathrates [8] is excluded in the present case. We



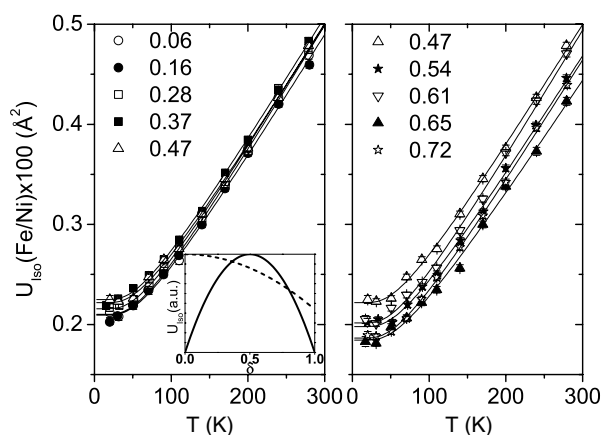


**Figure 6.** Temperature dependence of the Fe/Ni isotropic atomic displacement parameters for  $\text{Ce}_\delta\text{Fe}_{4-x}\text{Ni}_x\text{Sb}_{12}$ . The lines are guides to the eyes. The inset on the left panel displays the expected variations of static disorder as a function of  $\delta$  in the case of a Ce–vacancy effect (solid line) and Fe/Ni substitution (dotted line). The measured Ce filling fractions are displayed with corresponding symbols.

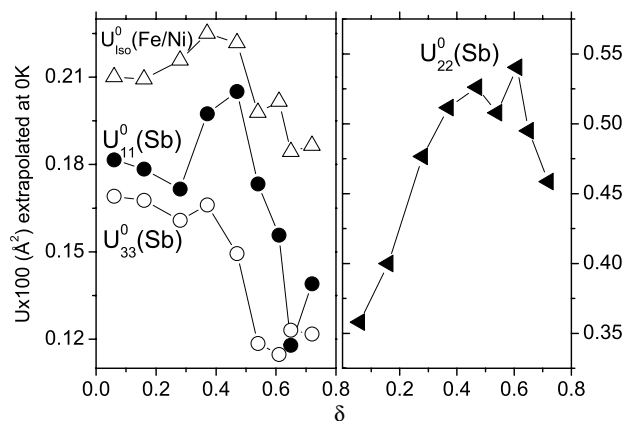


**Figure 7.** Dependence on the Ce filling fraction ( $\delta$ ) of thermal parameters extrapolated to 0 K for the Fe/Ni site (isotropic) and Sb site (anisotropic).

would also like to emphasize that the analysis reported here does not overestimate the static disorder as the zero-point motion is taken into account in the Einstein oscillator model. This treatment leads to results very similar than what is derived from the approach of Housley and Hess [20] (see [21] and references therein). For example the maximal dynamic contribution at 0 K was found to be  $0.0022 \text{ \AA}^2$  in 74% filled La samples [9] whereas the same analysis applied to the present systems leads to  $0.0020 \text{ \AA}^2$  for  $\delta = 0.72$ .

It is crucial to discuss, in addition to the positional disorder of Ce, the disorder of other atoms in the structure. Also, one should separate the effects caused by Ce disorder on one hand and by M disorder, i.e. Fe/Ni substitution, on the other. A quantitative analysis of the dynamic and static terms for these atoms is not as straightforward as before because the Einstein model is not a valid approximation. However, the inspection of the thermal parameters extrapolated to 0 K is extremely valuable for a qualitative understanding of the disorder since the ADP are

directly related to the phonon spectra (as they correspond to the projection of all the modes on a particular site). The temperature dependence of the ADP of the M atoms ( $M = \text{Fe/Ni}$ ) is displayed in figure 6 for all values of  $\delta$ . The dynamic contribution remains unchanged as seen from the similar slopes in the high temperature part of the plots. However, a slight variation of the thermal parameter extrapolated to 0 K ( $U_{\text{Iso}}^0(\text{Fe/Ni})$ ) is observed. The value increases by only a few per cent with increasing values of  $\delta$  in the range  $0.06 \leq \delta \leq 0.47$  and shows a more pronounced variation in the range  $0.47 \leq \delta \leq 0.72$  where it decreases by 20% (figure 7). This behaviour is inconsistent with static disorder caused by the Fe/Ni substitution alone because in that case, one would expect a continuous decrease across the entire composition range as shown by the dotted line in the inset of figure 6. This is simply due to the fact that the maximum static disorder is expected for a ratio Fe/Ni of 1 which corresponds to  $\delta = 0.0$ . On the other hand, if the disorder on the M site was the consequence of the Ce static disorder only, the dependence on  $\delta$  would follow the solid line (inset of figure 6). It is clear that the observed behaviour can only be explained by combining the two effects. Furthermore, the slight increase observed below  $\delta = 0.47$  seems to indicate that the role played by Ce disorder is weak compared to that of the intrinsic static disorder attributable to the Fe/Ni substitution.

Of particular interest is the evolution of the Sb thermal parameters, because these atoms play a central role in the thermal properties of filled skutterudites as explained by Feldmann [3]. As nearest neighbours they are more likely to be affected by the disorder on the cerium site than Fe or Ni are. Also, the disorder on the M site should directly affect the Sb atoms because of the covalent nature of the M–Sb bond. Figure 8, shows the temperature dependence of three components of the Sb anisotropic ADP for all samples (the off-diagonal term  $U_{23}$  is not represented; as its magnitude is much less than those of other terms, it is difficult to assess whether the variation is statistically significant). In a first approximation,  $\delta$  has no influence on the dynamic part as seen from the slopes of the curves at high temperature but, interestingly, it affects the static contribution of each component of the tensor in a different way. Figure 7 shows the variation with  $\delta$  of the Sb thermal parameters extrapolated to 0 K (denoted as  $U_{ij}^0$ ). The two components  $U_{11}^0$  and  $U_{33}^0$  show a variation very similar to that of  $U_{\text{Iso}}^0(\text{Fe/Ni})$  at 0 K with a pronounced decrease for  $\delta$  greater than 0.5. In contrast,  $U_{22}$  increases by more than 45% for  $0.06 \leq \delta \leq 0.47$  but shows a very soft decrease for higher values of  $\delta$ . As mentioned in the previous section, the observed behaviours result potentially from the combination of two effects: disorder on the Ce site on one hand and disorder on the M site on the other.  $U_{11}$  and  $U_{33}$  show a variation similar to that observed for the isotropic ADP of M and therefore are mainly the consequence of disorder on the Fe/Ni site. This is in agreement with the crystal symmetry showing that  $U_{11}$  and  $U_{33}$  are in-plane components along the M–Sb bond. In contrast,  $U_{22}$  varies similarly to the Ce isotropic ADP at low temperature (figure 4) and is found to be directly correlated with the disorder on the Ce site. This result is also in agreement with the symmetry because the component  $U_{22}$ , pointing along the Sb–Sb(2) bond towards the Ce atom, is expected to be greatly influenced by any disorder of this kind.

Overall, the picture that emerges from this study is more complex than the simple description of a rattling ion, in an oversized  $\text{Sb}_{12}$  cage, that has very little influence on the host network. It turns out that disorder effects cannot be neglected for partially filled skutterudites of the type investigated here because the partial filling of the voids by cerium induces a substantial static disorder of the cerium atom in addition to the large dynamic motion. The substitution of Ni for Fe also affects the structure by creating static disorder on the metal site, though with smaller magnitude. The Sb ADP reflects the effects of disorder from each sublattice (Ce and Fe/Ni). The Sb positional disorder is mainly a consequence of the Ce disorder which tends to distort the  $\text{Sb}_4$  rectangular rings along the axis corresponding to the longer Sb–Sb bond. The disorder along the shorter Sb–Sb distance is found to be negligible. An additional

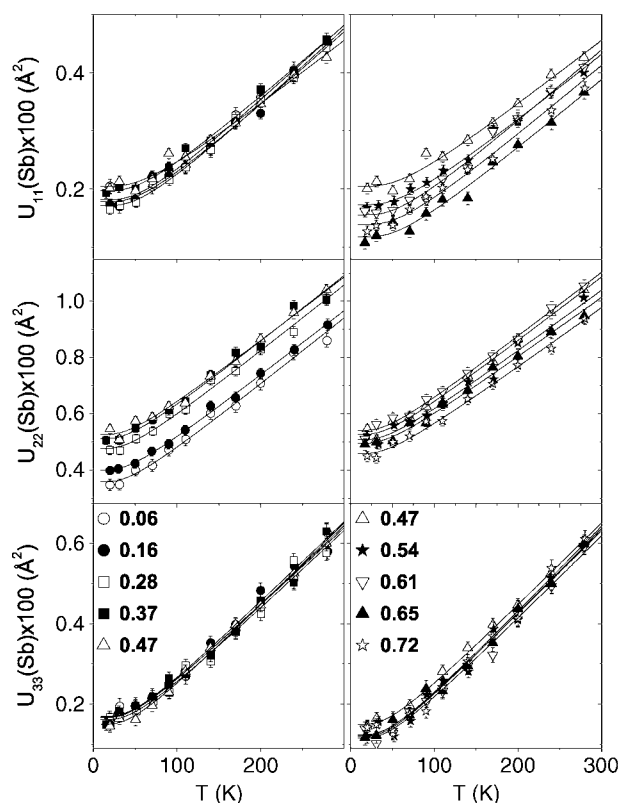


**Figure 8.** Anisotropic atomic displacement parameter of Sb versus temperature for  $\text{Ce}_\delta\text{Fe}_{4-x}\text{Ni}_x\text{Sb}_{12}$ :  $U_{11}$  (top panels),  $U_{22}$  (middle panels) and  $U_{33}$  (bottom panels). The measured Ce filling fractions are displayed with corresponding symbols.

distortion is caused by the disorder on the metallic site which increases the components of the ADP perpendicular to  $U_{22}$ . Consequently most of the vibration modes involving Sb atoms should be affected by these disorder effects. The model presented here suggests that instead of a unique force constant characterizing each of the interactions, the systems should show a distribution of force constants over a frequency range that is proportional to the amounts of both static disorders. This is in agreement with recent results [14] showing that most of the Raman- and infrared-active modes are quite broad for a La partially filled skutterudite. To go further in the study of disorder effects, it would be extremely valuable to model the disorder in these systems with lattice dynamics simulations using large supercells and calculate the atomic displacement parameters accordingly.

#### 4. Conclusion

The structural properties of the partially filled skutterudites  $\text{Ce}_\delta\text{Fe}_{4-x}\text{Ni}_x\text{Sb}_{12}$  have been systematically studied over a wide range of compositions  $\delta$ . We found a substantial static disorder of the cerium atom for compositions close to  $\delta = 0.5$  evidenced by large values of the atomic displacement parameters at low temperature. This disorder greatly affects the Sb nearest neighbours, in particular the  $U_{22}$  component of the anisotropic ADP. The substitution of Ni for Fe induces also static disorder on the Fe/Ni site that affects the other components of

the Sb thermal ellipsoid. These results show that, in addition to dynamic effects, positional disorder is a crucial parameter to consider when studying the physics and thermal properties of these compounds for compositions near half-filling.

### Acknowledgments

This work was supported by the European Community under the Framework Programme 5 IHP—Access to Research Infrastructures—ISIS Neutrons. We would like to thank Jon Bones of the ISIS user support group for technical support during the experiment.

### References

- [1] Sales B C, Mandrus D and Williams R K 1996 *Science* **272** 1325
- [2] Slack G A 1995 *CRC Handbook of Thermoelectrics* ed D M Rowe (Boca Raton, FL: Chemical Rubber Company) chapter 34, p 407
- [3] Feldman J L, Singh D J, Mazin I I, Mandrus D and Sales B C 2000 *Phys. Rev. B* **61** R9209
- [4] Chen B, Xu J-H, Uher C, Morelli D T, Meisner G P, Fleurial J-P, Caillat T and Borschchevsky A 1997 *Phys. Rev. B* **55** 1476
- [5] Grytsiv A *et al* 2002 *Phys. Rev. B* **66** 094411
- [6] Meisner G P, Morelli D T, Hu S, Yang J and Uher C 1998 *Phys. Rev. Lett.* **80** 3551
- [7] Nolas G S, Cohn J L and Slack G A 1998 *Phys. Rev. B* **58** 164
- [8] Sales B C, Chakoumakos B C, Jin R, Thompson J R and Mandrus D 2001 *Phys. Rev. B* **63** 245113
- [9] Chakoumakos B C, Sales B C, Mandrus D and Keppens V 1999 *Acta Crystallogr. B* **55** 341
- [10] Keppens V, Mandrus D, Sales B C, Chakoumakos B C, Dai P, Coldea R, Maple M B, Gajewski D A, Freeman E J and Bennington S 1998 *Nature* **395** 876
- [11] Cao D, Bridges F, Chesler P, Bushart S, Bauer E D and Maple M B 2004 *Phys. Rev. B* **70** 094109
- [12] Sales B C, Mandrus D, Chakoumakos B C, Keppens V and Thompson J R 1997 *Phys. Rev. B* **56** 15081
- [13] Sales B C, Chakoumakos B C and Mandrus D 2000 *Phys. Rev. B* **61** 2475
- [14] Feldman J L, Singh D J, Kendziora C, Mandrus D and Sales B C 2003 *Phys. Rev. B* **68** 094301
- [15] Larson A C and Von Dreele R B 1986 GSAS Generalized Structural Analysis System *Report LAUR-86-748* Los Alamos National Laboratory, Los Alamos, New Mexico, USA
- [16] Wang X-L, Wang Y D and Richardson J W 2002 *J. Appl. Crystallogr.* **35** 533
- [17] Chapon L, Ravot D and Tedenac J-C 1999 *J. Alloys Compounds* **282** 58
- [18] Chapon L, Ravot D and Tedenac J-C 2000 *J. Alloys Compounds* **299** 68
- [19] Hermann R P, Jin R, Schweika W, Grandjean F, Mandrus D, Sales B C and Long G J 2003 *Phys. Rev. Lett.* **90** 135505
- [20] Housley R M and Hess F 1966 *Phys. Rev.* **146** 517
- [21] Argyriou D N 1994 *J. Appl. Crystallogr.* **27** 155